Fermi National Accelerator Laboratory

DESY 95–114
FERMILAB-PUB-95/154-T
MPI/PhT/95-54
hep-ph/9506437
June 1995

ISSN 0418-9833

Neutral-Kaon Production in e^+e^-, ep, and $p\bar{p}$ Collisions at Next-to-Leading Order

J. Binnewies[1], B.A. Kniehl[2*], and G. Kramer[1]
[1] II. Institut für Theoretische Physik[†], Universität Hamburg
Luruper Chaussee 149, 22761 Hamburg, Germany
[2] Theoretical Physics Department, Fermi National Accelerator Laboratory
P.O. Box 500, Batavia, IL 60510, USA

Abstract

We present new sets of fragmentation functions for neutral kaons, both at leading and next-to-leading order. They are fitted to data on inclusive K^0 production in e^+e^- annihilation taken by MARK II at PEP ($\sqrt{s} = 29$ GeV) and by ALEPH at LEP. Our fragmentation functions lead to a good description of other e^+e^- data on inclusive K^0 production at various energies. They also nicely agree with the K^0_S transverse-momentum spectra measured by H1 at the DESY ep collider HERA, by UA5 at the CERN $Sp\bar{p}S$ Collider, and by CDF at the Fermilab Tevatron.

*Permanent address: Max-Planck-Institut für Physik, Werner-Heisenberg-Institut, Föhringer Ring 6, 80805 Munich, Germany.

†Supported by Bundesministerium für Forschung und Technologie, Bonn, Germany, under Contract 05 6 HH 93P (5), and by EEC Program *Human Capital and Mobility* through Network *Physics at High Energy Colliders* under Contract CHRX-CT93-0357 (DG12 COMA).

Operated by Universities Research Association Inc. under contract with the United States Department of Energy

1 Introduction

Recently, precise data on inclusive $\pi^{\pm}$, $K^{\pm}$, and unspecified-charged-hadron production in e^+e^- annihilation at the Z resonance has been published. Using this new data and similar data from lower centre-of-mass (CM) energy ($\sqrt{s} = 29$ GeV), we constructed new sets of fragmentation functions (FF) for charged pions and kaons at leading order (LO) and next-to-leading order (NLO) [1]. These new parameterizations were tested against data on $\pi^{\pm}$, $K^{\pm}$, and charged-hadron production in e^+e^- annihilation at various energies and data on single-charged-hadron production in small-Q^2 ep scattering at HERA, which presents a nontrivial check of the factorization theorem of the QCD-improved parton model.

Besides charged pions and kaons or just charged hadrons, K^0_S mesons are easily detected through their dominant decay into $\pi^+\pi^-$ pairs. The ALEPH [2], DELPHI [3], OPAL [4], and L3 [5] Collaborations at LEP have recently reported on their high-statistics analyses of inclusive single K^0 production.[1]

Following our strategy of constructing FF for charged pions and kaons, we shall combine this new data on K^0 production at the Z resonance with the rather precise data taken at $\sqrt{s} = 29$ GeV by the MARK II Collaboration [6] at PEP to obtain FF for the neutral kaons. Owing to the factorization theorem, the same FF can be used to predict cross sections of inclusive single K^0 production at high transverse momenta (p_T) in other processes like ep and $p\bar{p}$ scattering. The functions characterizing the fragmentation of gluons, u, d, s, c, and b quarks (antiquarks) into neutral kaons contribute quite differently in these processes as compared to e^+e^- annihilation. For example, in e^+e^- annihilation at the Z resonance, all five quarks are directly produced, whereas the gluon does not directly couple to the electroweak currents. The gluon only contributes in higher orders and mixes with the quarks through the Q^2 evolution. On the other hand, in the case of inclusive light-meson production at moderate p_T in high-energy $p\bar{p}$ collisions, the cross section is dominated by gluon fragmentation [7]. In ep collisions with almost real photons at HERA, the situation is mixed. In the lower p_T range ($p_T \lesssim 15$ GeV), inclusive single hadron production proceeds dominantly via the resolved photoproduction processes $gg \to gg$, $qg \to gq$, and $qg \to qg$, where the first and second partons originate from the virtual photon and the proton, respectively, while the third one fragments into the outgoing hadron [8]. Direct photoproduction only plays a significant rôle at larger p_T [9]. Therefore, quark and gluon fragmentation should give comparable contributions even at small p_T.

In our previous work on FF for charged pions and kaons [1], we could exploit the information from tagged three-jet events in e^+e^- annihilation to constrain the gluon fragmentation into charged hadrons, which constrained also that into charged pions and kaons. Unfortunately, such information is not yet available for inclusive K^0 production in e^+e^- annihilation. Thus, we shall have to resort to the information on gluon fragmentation into charged kaons which we extracted in Ref. [1].

[1] Unless stated otherwise, we shall collectively use the symbol K^0 for the sum of K^0_S and K^0_L (or K^0 and $\overline{K}^0$).

Another problem that requires special attention is related to the distinction of the different quark flavours in K^0 fragmentation. In our recent analysis of $\pi^\pm$ and $K^\pm$ fragmentation [1], we had some information on the fragmentation of specific flavours at our disposal. Preliminary measurements of charged-hadron production by the ALEPH Collaboration [10] distinguished between three cases, namely the fragmentation of (i) u, d, s quarks, (ii) b quarks only, and (iii) all five flavours (u, d, s, c, and b). This enabled us to remove the assumption that the s, c, and b quarks fragment into charged pions (kaons) in the same way, which we had made in our earlier work [11]. Although equivalent information is still lacking for K^0 fragmentation in e^+e^- annihilation, we shall follow the approach of our recent work on $\pi^\pm$ and $K^\pm$ production [1], where no additional identities between the FF of different quark flavours were imposed, except those following from the flavour content of the produced mesons. Should it turn out that the relative importance of the different flavours cannot yet be pinned down so reliably, then this will not be due to a shortcoming of this specific procedure; this would just signal that more detailed data is indispensable in order to determine the differences in flavour of the FF more accurately, leaving room for further improvements.

It is the purpose of this work to make use of the new K^0 data by ALEPH [2] together with the K^0 data by MARK II [6] to construct new LO and NLO sets of FF, only identifying the FF of the d and s quarks and imposing no constraints on the quarks otherwise. At the starting scale, Q_0, we shall take the gluon FF of the neutral kaons to be equal to their charged counterparts. The recent data from DELPHI [3], OPAL [4], and L3 [5] agree with the ALEPH data and will not be used in our fit. A comparison of all four data sets may be found in a report by OPAL [4]. We choose the ALEPH data, since, in the region of relatively large x, which we are mainly interested in, it has a slightly smaller total error than the data from DELPHI and OPAL. The data from L3 does not extend to x values in excess of 0.24 and is thus less useful for our purposes.

Our new K^0 FF sets will be tested against older data from e^+e^- colliders with lower CM energies. Furthermore, we shall calculate the p_T distributions of K^0_S mesons produced inclusively in ep and $p\bar{p}$ collisions at various CM energies and compare them with preliminary H1 data [12] and with data from UA5 [13] and CDF [14], in order to check whether the gluon fragmentation and the relative importance of the various quark flavours are realistically described.

An alternative way of constructing FF is to fit to data generated by well-established Monte Carlo event generators rather than experimental data. This avenue has just recently been taken in Ref. [15], where, among other things, a NLO set of K^0_S FF has been presented. This offers us yet another opportunity to test our K^0 FF, namely against Monte Carlo output. We shall report the outcome of such a comparison later on.

The LO and NLO formalisms for extracting FF from e^+e^- data are comprehensively described in our previous works [1,11] and will not be reviewed here. Also, the formulae that are needed to calculate the cross sections of inclusive single hadron production in ep collisions (with almost real photons) and in $p\bar{p}$ collisions may be found in earlier publications [1,8,9]. The NLO formulae in these references are based on the works by Aversa *et al.* [16] (resolved photoproduction and $p\bar{p}$ collisions), Aurenche *et al.* [17]

(direct photoproduction), and Altarelli *et al.* [18] (e^+e^- collisions).

This paper is organized as follows. In Sect. 2, we shall describe the actual analysis and present our results for the K^0 FF. We shall also check these FF against e^+e^- data at lower energies which we did not use in our fits. Furthermore, we shall compare the calculated inclusive K^0_S cross sections for ep and $p\bar{p}$ collisions with H1, UA5, and CDF experimental results. Our conclusions will be summarized in Sect. 3. In the Appendix, we shall list simple parameterizations of our FF sets for inclusive K^0 production.

2 Results

For our analysis, we select the data on K^0 production taken at energy $\sqrt{s} = 29$ GeV by the MARK II Collaboration at PEP [6] and those collected at $\sqrt{s} = M_Z$ by the ALEPH Collaboration at LEP [2]. This data comes in the form $(1/\sigma_{\rm had})d\sigma/dx$ as a function of $x = 2E_{K^0}/\sqrt{s}$, where $\sqrt{s}$ and E_{K^0} are the e^+e^- and K^0 energies in the CM system, respectively. The data from MARK II and ALEPH lie within the ranges $0.036 \leq x \leq 0.69$ and $0.003698 \leq x \leq 0.8187$, respectively. These and other e^+e^- experiments present inclusive cross sections for $K^0_S + K^0_L$ (or $K^0 + \overline{K}^0$), *i.e.*, the sum of the two individual rates. We adopt this convention, *i.e.*, our FF refer to the fragmentation of any given parton into K^0_S and K^0_L (or K^0 and $\overline{K}^0$). For the fitting procedure, we use the x bins in the interval between $x_{\rm min} = \max(0.1, 2\,{\rm GeV}/\sqrt{s})$ and $x_{\rm max} = 0.8$ and integrate the theoretical functions over the bin widths, which is equivalent to the experimental binning procedure. The restriction at small x is to exclude events in the non-perturbative region, where mass effects are important. Very-large-x data suffer from huge uncertainties, so we prefer to disregard the few data-points above $x_{\rm max}$. As usual, we parameterize the x dependence of the FF at the starting scale Q_0 as

$$D_a^{K^0}(x, Q_0^2) = N x^\alpha (1-x)^\beta, \tag{1}$$

where a stands for any quark flavour or the gluon. We impose the condition $D_s^{K^0+\overline{K}^0}(x, Q^2) = D_d^{K^0+\overline{K}^0}(x, Q^2)$. For all the other quark FF, we take N, α, and β to be independent fit parameters.

As mentioned above, the e^+e^- data on inclusive single particle production does not well constrain the gluon FF, which, however, plays an important rôle in ep reactions and even more so in $p\bar{p}$ processes. Since, at present, there exists no additional information on gluon fragmentation to neutral kaons in e^+e^- annihilation, we fall back on the results on the fragmentation of gluons into charged kaons obtained in our recent analysis [1]. We argue that the supposedly flavour-blind gluon should fragment into charged and neutral kaons at the same rate, and identify the corresponding FF. Later on in this section, we shall demonstrate in more detail that, in want of better data, this is a sensible prescription.

Of course, the data on $\pi^\pm$ and $K^\pm$ production have much better statistics than the K^0 production data under investigation in this paper. For this reason, and for compatibility with our $\pi^\pm$ and $K^\pm$ sets, we do not fit $\Lambda_{\overline{\rm MS}}$ anew, but adopt the values determined in

Ref. [1], $\Lambda^{(5)}_{\overline{\rm MS}} = 107$ MeV (195 MeV) in LO (NLO). We are thus left with 12 independent fit parameters.

The quality of the fit is measured in terms of the $\chi^2_{\rm d.o.f.}$ for all selected data points. The technical procedure to determine these 12 parameters, using well-tested numerical techniques of multidimensional optimization [19], is similar to our earlier work [1]. As in Ref. [1], we choose $Q_0 = \sqrt{2}$ GeV for the u, d, and s quarks, $Q_0 = m(\eta_c) = 2.9788$ GeV [20] for the c quark, and $Q_0 = m(\Upsilon) = 9.46037$ GeV [20] for the b quark. Our results are listed below. For the sum of K^0 and $\overline{K}^0$, we find

$$\begin{aligned}
D_u^{(K^0+\overline{K}^0,\,\rm LO)}(x,Q_0^2) &= 0.51\,x^{-0.841}\,(1-x)^{1.55},\\
D_d^{(K^0+\overline{K}^0,\,\rm LO)}(x,Q_0^2) &= D_s^{(K^0+\overline{K}^0,\,\rm LO)}(x,Q_0^2) = 1.47\,x^{-0.691}\,(1-x)^{3.49},\\
D_c^{(K^0+\overline{K}^0,\,\rm LO)}(x,Q_0^2) &= 1.00\,x^{-0.738}\,(1-x)^{2.93},\\
D_b^{(K^0+\overline{K}^0,\,\rm LO)}(x,Q_0^2) &= 0.68\,x^{-0.598}\,(1-x)^{1.93},\\
D_g^{(K^0+\overline{K}^0,\,\rm LO)}(x,Q_0^2) &= 0.43\,x^{-0.374}\,(1-x)^{2.69}
\end{aligned} \tag{2}$$

in LO and

$$\begin{aligned}
D_u^{(K^0+\overline{K}^0,\,\rm NLO)}(x,Q_0^2) &= 0.50\,x^{-0.781}\,(1-x)^{1.58},\\
D_d^{(K^0+\overline{K}^0,\,\rm NLO)}(x,Q_0^2) &= D_s^{(K^0+\overline{K}^0,\,\rm NLO)}(x,Q_0^2) = 1.25\,x^{-0.564}\,(1-x)^{3.33},\\
D_c^{(K^0+\overline{K}^0,\,\rm NLO)}(x,Q_0^2) &= 0.99\,x^{-0.601}\,(1-x)^{3.80},\\
D_b^{(K^0+\overline{K}^0,\,\rm NLO)}(x,Q_0^2) &= 0.53\,x^{-0.571}\,(1-x)^{1.98},\\
D_g^{(K^0+\overline{K}^0,\,\rm NLO)}(x,Q_0^2) &= 0.33\,x^{-0.351}\,(1-x)^{0.65}
\end{aligned} \tag{3}$$

in NLO. Here, it is understood that the Q_0^2 values refer to the individual starting points given above. For the data that we fitted to, we find very small $\chi^2_{\rm d.o.f.}$ values, namely 0.53 (0.52) at NLO (LO). The $\chi^2_{\rm d.o.f.}$ values achieved for the various data sets may be seen from Table I. Our FF also give a good description of the Z-resonance data from DELPHI [3] and OPAL [4], which yield just slightly larger values of $\chi^2_{\rm d.o.f.}$ The same is true for the lower-energy data taken by CELLO [21] and TASSO [22] at PETRA ($\sqrt{s} = 35$ GeV) and for the data collected by HRS [23] and TPC [24] at PEP ($\sqrt{s} = 29$ GeV). Among the data that we compared with, those from CLEO [25] and ARGUS [26] have the lowest energy ($\sqrt{s} = 10$ GeV). Only the ARGUS data give an exceptionally large $\chi^2_{\rm d.o.f.}$, of order 5.

For the reader's convenience, we list simple parameterizations of the x and Q^2 dependences of our K^0 FF sets in the Appendix. We believe that such parameterizations are indispensable for practical purposes, especially at NLO. However, we should caution the reader that these parameterizations describe the evolution of the FF only approximately. Deviations in excess of 8% may occur for $x < 0.1$ and for $Q > 100$ GeV, in particular for the gluon. While this kind of accuracy is fully satisfactory for most applications, it is insufficient for the comparison with the high-statistics data collected at LEP. We wish to point out that all $\chi^2_{\rm d.o.f.}$ values presented in this paper have been computed using FF with explicit Q^2 evolution, which have an estimated relative error of less than 0.4%.

TABLE I. CM energies, experimental collaborations, numbers of data points used, and $\chi^2_{\rm d.o.f.}$ values obtained at NLO and LO for the various e^+e^- data samples discussed in the text. The data used in the fits are marked by an asterisk.

$\sqrt{s}$ [GeV]	Experiment	Ref.	No. of points	$\chi^2_{\rm d.o.f.}$ in NLO	$\chi^2_{\rm d.o.f.}$ in LO
91.2	ALEPH *	[2]	9	0.60	0.57
	DELPHI	[3]	11	0.94	0.96
	OPAL	[4]	8	0.95	0.93
35.0	CELLO	[21]	6	0.23	0.23
	TASSO	[22]	10	1.84	1.74
29.0	MARK II *	[6]	11	0.48	0.49
	HRS	[23]	12	2.66	2.93
	TPC	[24]	6	0.41	0.43
10.49	CLEO	[25]	12	1.27	1.15
9.98	ARGUS	[26]	4	5.42	5.32

Since we have built in the $c\bar{c}$ and $b\bar{b}$ thresholds, we have three different starting scales Q_0. To illustrate the relative size of the FF for the different quark flavours and the gluon, we have plotted them in Fig. 1 as functions of x for $Q = 10$ GeV. We show only the NLO results. The pattern is somewhat unusual and, contrary to naïve expectations, not very similar to the $K^\pm$ FF in our earlier work [1]. The u-quark, b-quark, and gluon FF are rather hard, while the d/s-quark and the c-quark distributions are soft. This pattern is already visible at the starting scales Q_0 in Eqs. (2) and (3), where we must keep in mind, however, that the starting scale Q_0 takes on three distinct values for the light, c, and b quarks. Guided by our findings in connection with $K^\pm$ fragmentation, we would expect that, in Fig. 1, the d/s-quark FF should be hardest, and that the b-quark FF should resemble that of the c quark. At this stage, it cannot be excluded that the relative importance of the individual quark flavours will need some adjustment. But for this we would need additional e^+e^- data on inclusive K^0 production for which the fragmentation of the various quark flavours and the gluon is disentangled, similarly to what has been done in the case of charged-hadron production. Unfortunately, the existing information from ep and $p\bar{p}$ collisions does not help us much either. Due to its high threshold, b-quark production is absent at small p_T, below 9.5 GeV. In our ep analysis, $c/\bar{c}$ production accounts for 8% (10%) of the cross section at $p_T = 5$ (8) GeV, while, in our $p\bar{p}$ calculation for $\sqrt{s} = 1.8$ TeV, its contribution at the same p_T values is 0.7% (0.8%), *i.e.*, in both reactions it is small or negligible.

The goodness of our fits to the ALEPH [2] and MARK II [6] data may be judged from Fig. 2. At NLO (LO), we find $\chi^2_{\rm d.o.f.}$ values of 0.60 (0.57) for ALEPH and 0.48 (0.49) for MARK II.

The factorization theorem guarantees that the FF which we extracted from e^+e^- data may also be used to predict other types of inclusive single K^0 production cross sections, *e.g.*, for $\gamma\gamma$, ep, or hadron-hadron collisions. In the following, we shall present NLO predictions for inclusive photoproduction of K^0_S mesons at HERA and confront

them with preliminary data taken by H1 [12]. As in the H1 measurement, we shall consider the p_T spectrum of the produced K_S^0 mesons, averaged over the rapidity range $|y_{\rm lab}| < 1.5$. We shall work at NLO in the $\overline{\rm MS}$ scheme with $N_f = 5$ quark flavours, fix the renormalization and factorization scales by setting $\mu = M_\gamma = M_p = M_h = \xi p_T$, and adopt the NLO parton distribution functions (PDF) of the photon and the proton from Refs. [27] and [28], respectively, together with our NLO FF. We wish to emphasize that also the hard-scattering cross sections will be calculated up to NLO. We shall evaluate α_s to two loops with $\Lambda^{(5)}_{\overline{\rm MS}} = 158$ MeV [28]. The quasi-real photon spectrum will be simulated according to H1 conditions, by imposing the cut $0.3 < z < 0.7$ on $z = E_\gamma/E_e$ and choosing $Q^2_{\rm max} = 0.01$ GeV^2. Our predictions for $\xi = 1/2$, 1, and 2 are confronted with the H1 points in Fig. 3. The agreement is satisfactory as for both shape and normalization. Unfortunately, the H1 data are accumulated at rather small p_T ($p_T \leq 3$ GeV), whereas our predictions should be more reliable at larger p_T. We must keep in mind, however, that this represents the first measurement of inclusive K_S^0 production at HERA, based on data taken in 1993, and that the numbers are still preliminary. More data at larger p_T is expected to appear after the analysis of the 1994 run is completed. As we see in Fig. 3, the cross section shows only moderate scale dependence, which indicates relatively good perturbative stability. Notice that our prediction in Fig. 3 refers to K_S^0 production, which corresponds to the average of K^0 and $\overline{K}^0$.

There only exists rather limited experimental information on inclusive K_S^0 production in $p\bar{p}$ collisions. The only high-energy data available come from the UA5 Collaboration [13] at the CERN S$p\bar{p}$S Collider and from the CDF Collaboration [14] at the Fermilab Tevatron. In Fig. 4, we show our predictions for the p_T spectrum of $p\bar{p} \to K_S^0 + X$ at $\sqrt{s} = 200$, 546, and 900 GeV, with rapidity averaged over the interval $-2.5 < y < 2.5$. The calculation is performed at NLO in the $\overline{\rm MS}$ scheme with $N_f = 5$ quark flavours using the CTEQ3 proton PDF [28]. The renormalization and fragmentation scales are identified and set equal to $p_T/2$, p_T, and $2p_T$. The agreement with the UA5 data [13] is quite satisfactory. It is best for the highest CM energy. Unfortunately, this data is accumulated at rather small p_T. On average, the agreement is best with scales equal to p_T. The data from CDF [14] is more recent. It was taken at $\sqrt{s} = 630$ and 1800 GeV. This data together with our theoretical results for scales $p_T/2$, p_T, and $2p_T$ are plotted versus p_T in Fig. 5. The experimental and theoretical results are both averaged over $|y| < 1.0$. Unfortunately, the CDF data has rather small p_T, too. Again, the agreement of our calculation with the data is best for scales equal to p_T. Only at very small p_T, deviations from the data taken at $\sqrt{s} = 1800$ GeV are noticeable. This is to be expected, since the theoretical predictions are valid only for large p_T; their reliability at p_T below 1.5 GeV is certainly questionable. At this point, we would like to encourage our experimental colleagues in the CDF Collaboration to also analyze the vast amount of data collected after 1989 with respect to light-meson fragmentation. In view of the considerable recent theoretical progress in this field, this would be interesting and exciting in its own right, rather than but a boring measure to assess backgrounds for certain other processes which presently happen to be more en vogue. In fact, this would allow us to test the QCD-improved parton model and, in particular, the factorization theorem at the quantum

level.

Due to their limited p_T range and their modest accuracy, the data sets presented in Figs. 4 and 5 are not so well suited for constraining the FF obtained from the e^+e^- analysis. However, they provide a welcome cross check, in particular with respect to the gluon FF, which is only feebly constrained by the e^+e^- data. To elaborate this point, we investigate the influence of the gluon fragmentation on the ep and $p\bar{p}$ cross sections. To that end, we repeat the calculations of Figs. 3–5 switching off the quark FF. In Fig. 6, we show the outcome normalized to the full calculations for the ep cross section and the 200 GeV, 630 GeV, and 1800 GeV $p\bar{p}$ cross sections. We observe that, in the low-p_T range, the $p\bar{p}$ cross sections are overwhelmingly dominated by the gluon FF. The ratio increases with CM energy and reaches 90% at the largest energy. This shows that, if it were not for the large errors, the $p\bar{p}$ data would be perfectly well suited for constraining the gluon FF. Looking back at Figs. 4 and 5, it is fair to say that the strength of the gluon FF as obtained from our $e^+e^- \to h^\pm + X$ fits is large enough to account for the $p\bar{p}$ data. This is in accord with recent studies of inclusive charged-hadron production in $p\bar{p}$ collisions [29]. We also examined in which x range the gluon FF maximally contributes to the $p\bar{p}$ inclusive cross sections in the considered p_T range. Depending on the CM energy, the most important x values are concentrated around $x = 0.4$. This means that the $p\bar{p}$ data only constrains the gluon FF in a limited range of x. On the other hand, we know that the e^+e^- data does not determine the gluon FF very accurately, *i.e.*, a good description of the e^+e^- data may also be obtained with a weaker gluon FF. The ep data also need a sufficiently strong gluon FF, in particular to describe the data near $p_T = 2$ GeV. At larger p_T, the influence of the gluon FF diminishes, and the quark FF come into play much more strongly. This is to be expected, since, in the ep cross section, the $qg \to qg$ channel is similarly important as the $gg \to gg$ and $qg \to gq$ channels, even at small p_T.

Having established the importance of the gluon FF for K_S^0 production in $p\bar{p}$ collisions, we should take a closer look at our assumptions concerning the gluon FF. These were twofold. We explicitly stated that we were going to assume $D_g^{K^0}(x, Q_0) = D_g^{K^\pm}(x, Q_0)$ (a). A second, hidden assumption was that $D_g^{K^\pm}$ had been well constrained by our previous analysis [1], although only experimental information on the gluon FF for the sum of the charged hadrons had been available (b). By investigating the ratio of the cross section for inclusive kaon production in hadron collisions to that for charged hadrons, we may check both assumptions. For one thing, this ratio is approximately equal to the ratio of the respective gluon FF (at least for high CM energies), which enables us to test (b). On the other hand, this ratio has been measured for both charged and neutral kaons, providing us with a check of (a). In Fig. 7, we confront our predictions, based on assumptions (a) and (b), with the experimental data on neutral-kaon production in 1.8 TeV $p\bar{p}$ collisions by CDF [14] and on charged-kaon production in 53 GeV and 27 GeV pp scattering by the British–Scandinavian Collaboration [30] at the CERN ISR and by the Chicago–Princeton Collaboration [31] at Fermilab, respectively. In the theoretical calculation of charged-hadron production, only charged pions and kaons are included. Protons, Λ hyperons, and other heavy hadrons are known to contribute little to the cross section and are neglected here. We find throughout good agreement with the data. All data, as well as

our predictions, approach a plateau at not-too-small p_T. Its height is about 0.2, fairly independently of the CM energy or whether neutral or charged kaons are considered.

At this point, we should compare our results on the K^0 FF with those obtained in Ref. [15]. The cross section of inclusive K_S^0 production at $\sqrt{s} = 1.8$ TeV under CDF conditions as predicted by Ref. [15] agrees reasonably well with our own calculation; it ranges between 50% and 70% of our result for p_T between 2 and 7 GeV.

These tests reassure us of the soundness of the assumptions concerning the gluon FF of the neutral kaons which we had to make in view of shortcomings in the presently available experimental information. From a theoretical point of view, it would certainly be desirable to constrain the K^0 FF by using just e^+e^- data, as this would enable us to test them in other types of processes so as to probe the factorization theorem. Unfortunately, this is not yet possible, which has led us to use additional input to obtain FF that satisfactorily describe a variety of e^+e^-, ep, and $p\bar{p}$ data.

3 Summary and Conclusions

We presented FF for neutral kaons, both at LO and NLO. They were constructed from fits to data on inclusive $K^0 + \overline{K}^0$ production in e^+e^- annihilation taken by MARK II [6] at PEP ($\sqrt{s} = 29$ GeV) and by ALEPH at LEP [2]. Although our FF were only fitted to the MARK II and ALEPH data, it turned out that they lead to an excellent description of other e^+e^- data on inclusive $K^0 + \overline{K}^0$ production ranging from $\sqrt{s} = 10$ GeV to LEP energy. We always obtained $\chi^2_{\text{d.o.f.}}$ values of order unity. The only exception, with $\chi^2_{\text{d.o.f.}} \approx 5$, occurred for the ARGUS data at $\sqrt{s} = 9.98$ GeV.

Since the e^+e^- data do not constrain the gluon FF so well, we made NLO predictions for the p_T spectra of K_S^0 mesons produced inclusively in the scattering of quasi-real photons on protons under HERA conditions and in proton-antiproton collisions under UA5 and CDF conditions, and confronted them with the respective data. The agreement turned out to be quite satisfactory. We discovered that the gluon FF is very important to account for the $p\bar{p}$ data. We are thus faced with the unfortunate situation that the $p\bar{p}$ data almost exclusively tests the gluon FF, which is of little relevance for existing e^+e^- data. Vice versa, the quark FF, which—up to a residual uncertainty in the relative importance of the individual flavours—are fixed by a wealth of e^+e^- data, have hardly any impact on $p\bar{p} \to K_S^0 + X$. The situation will be ameliorated as soon as the ep scattering experiments at HERA provide us with higher-statistics data, in particular at larger p_T. In conclusion, present data does not yet allow us to test the universality of the FF in inclusive K^0 production; the situation rather requires that we exploit the universality postulated by the factorization theorem in order to extract meaningful FF. This was achieved in the work presented here.

In order to make further progress, one would need e^+e^- data on inclusive K^0 production in which the different quark flavours are tagged. Also, the gluon FF would have to be constrained better, *e.g.*, by studying inclusive K^0 production in tagged three-jet events or by measuring the longitudinal part of the cross section, similarly to what has been

done for charged particles. As for ep and $p\bar{p}$ collisions, data at larger p_T with sufficient accuracy would be highly welcome, since they would allow us to quantitatively test the factorization theorem of fragmentation in the QCD-improved parton model.

ACKNOWLEDGMENTS

We are grateful to Frank Linsel for making available to us the preliminary H1 data on inclusive photoproduction of neutral kaons prior to their official publication [12]. We thank Simona Rolli for providing us with numerical results obtained on the basis of Ref. [15] and for useful discussions. One of us (BAK) is indebted to the FNAL Theory Group for inviting him as a Guest Scientist and for the great hospitality extended to him.

A Parameterizations

For the reader's convenience, we shall present here simple parameterizations of the x and Q^2 dependence of our FF.[2] As usual, we introduce the scaling variable

$$\bar{s} = \ln \frac{\ln (Q^2/\Lambda^2)}{\ln (Q_0^2/\Lambda^2)}. \tag{4}$$

For Λ we use the $\overline{\mathrm{MS}}$ value appropriate to $N_f = 5$ flavours, since the parameterization would not benefit from the incorporation of discontinuities in $\bar{s}$. $\Lambda^{(5)}_{\overline{\mathrm{MS}}}$ is taken from our previous fit [1] to be 107 MeV (195 MeV) in LO (NLO). Similarly to Eqs. (2)–(3), we use three different values for Q_0, namely

$$Q_0 = \begin{cases} \sqrt{2}\ \mathrm{GeV}, & \text{if} \quad a = u, d, s, g \\ m(\eta_c) = 2.9788\ \mathrm{GeV}, & \text{if} \quad a = c \\ m(\Upsilon) = 9.46037\ \mathrm{GeV}, & \text{if} \quad a = b \end{cases} . \tag{5}$$

This leads to three different definitions of $\bar{s}$. For definiteness, we use the symbol $\bar{s}_c$ for charm and $\bar{s}_b$ for bottom along with $\bar{s}$ for the residual partons.

We parameterize our FF by simple functions in x with coefficients which we write as polynomials in $\bar{s}$, $\bar{s}_c$, and $\bar{s}_b$. We find that the template

$$D(x, Q^2) = N x^{\alpha} (1 - x)^{\beta} \tag{6}$$

is sufficiently flexible, except for $D_g^{(K^0+\overline{K}^0,\mathrm{NLO})}$, where we include an additional factor $(1+\gamma/x)$ on the right-hand side of Eq. (6). For $\bar{s} = \bar{s}_c = \bar{s}_b = 0$, the parameterizations agree with the respective ansätze in Eqs. (2)–(3). The charm and bottom parameterizations must be put to zero by hand for $\bar{s}_c < 0$ and $\bar{s}_b < 0$, respectively.

We list below the parameters to be inserted in Eq. (6) both at LO and NLO. The resulting parameterizations correctly describe the Q^2 evolution up to 8% for $Q_0 \leq Q \leq 100$ GeV and $0.1 \leq x \leq 0.8$.

[2] A FORTRAN subroutine that returns the FF for given x and Q^2 may be obtained from the authors via e-mail (binnewie@ips107.desy.de, kniehl@vms.mppmu.mpg.de).

1. LO FF for $(K^0 + \overline{K}^0)$:

- $D_u^{(K^0+\overline{K}^0,\mathrm{LO})}(x, Q^2)$:

$$\begin{aligned} N &= 0.510 - 0.251\bar{s} + 0.036\bar{s}^2 \\ \alpha &= -0.841 - 0.285\bar{s} + 0.021\bar{s}^2 \\ \beta &= 1.550 + 0.712\bar{s} - 0.069\bar{s}^2 + 0.037\bar{s}^3 \end{aligned} \tag{7}$$

- $D_d^{(K^0+\overline{K}^0,\mathrm{LO})}(x, Q^2) = D_s^{(K^0+\overline{K}^0,\mathrm{LO})}(x, Q^2)$:

$$\begin{aligned} N &= 1.470 - 1.088\bar{s} + 0.276\bar{s}^2 \\ \alpha &= -0.691 - 0.312\bar{s} - 0.045\bar{s}^2 + 0.038\bar{s}^3 \\ \beta &= 3.490 + 0.851\bar{s} - 0.181\bar{s}^2 + 0.098\bar{s}^3 \end{aligned} \tag{8}$$

- $D_c^{(K^0+\overline{K}^0,\mathrm{LO})}(x, Q^2)$:

$$\begin{aligned} N &= 1.000 - 0.679\bar{s}_c + 0.111\bar{s}_c^2 + 0.058\bar{s}_c^3 \\ \alpha &= -0.738 - 0.302\bar{s}_c - 0.073\bar{s}_c^2 + 0.084\bar{s}_c^3 \\ \beta &= 2.930 + 0.758\bar{s}_c - 0.118\bar{s}_c^2 + 0.107\bar{s}_c^3 \end{aligned} \tag{9}$$

- $D_b^{(K^0+\overline{K}^0,\mathrm{LO})}(x, Q^2)$:

$$\begin{aligned} N &= 0.680 - 0.470\bar{s}_b + 0.241\bar{s}_b^2 - 0.115\bar{s}_b^3 \\ \alpha &= -0.598 - 0.407\bar{s}_b + 0.059\bar{s}_b^2 + 0.063\bar{s}_b^3 \\ \beta &= 1.930 + 0.554\bar{s}_b + 0.232\bar{s}_b^2 - 0.186\bar{s}_b^3 \end{aligned} \tag{10}$$

- $D_g^{(K^0+\overline{K}^0,\mathrm{LO})}(x, Q^2)$:

$$\begin{aligned} N &= 0.430 - 0.881\bar{s} + 0.860\bar{s}^2 - 0.320\bar{s}^3 \\ \alpha &= -0.374 - 2.147\bar{s} + 1.239\bar{s}^2 - 0.232\bar{s}^3 \\ \beta &= 2.690 + 1.515\bar{s} - 0.188\bar{s}^2 - 0.071\bar{s}^3 \end{aligned} \tag{11}$$

2. NLO FF for $(K^0 + \overline{K}^0)$:

- $D_u^{(K^0+\overline{K}^0,\mathrm{NLO})}(x, Q^2)$:

$$\begin{aligned} N &= 0.500 - 0.125\bar{s} - 0.051\bar{s}^2 \\ \alpha &= -0.781 - 0.500\bar{s} + 0.264\bar{s}^2 - 0.133\bar{s}^3 \\ \beta &= 1.580 + 1.074\bar{s} - 0.380\bar{s}^2 + 0.084\bar{s}^3 \end{aligned} \tag{12}$$

- $D_d^{(K^0+\overline{K}^0,\mathrm{NLO})}(x,Q^2) = D_s^{(K^0+\overline{K}^0,\mathrm{NLO})}(x,Q^2)$:

$$\begin{aligned} N &= 1.250 - 1.385\bar{s} + 0.896\bar{s}^2 - 0.251\bar{s}^3 \\ \alpha &= -0.564 - 0.718\bar{s} + 0.208\bar{s}^2 \\ \beta &= 3.330 + 0.100\bar{s} + 0.388\bar{s}^2 - 0.064\bar{s}^3 \end{aligned} \tag{13}$$

- $D_c^{(K^0+\overline{K}^0,\mathrm{NLO})}(x,Q^2)$:

$$\begin{aligned} N &= 0.990 - 1.020\bar{s}_c + 0.639\bar{s}_c^2 - 0.199\bar{s}_c^3 \\ \alpha &= -0.601 - 0.666\bar{s}_c + 0.189\bar{s}_c^2 \\ \beta &= 3.800 + 0.192\bar{s}_c + 0.382\bar{s}_c^2 - 0.077\bar{s}_c^3 \end{aligned} \tag{14}$$

- $D_b^{(K^0+\overline{K}^0,\mathrm{NLO})}(x,Q^2)$:

$$\begin{aligned} N &= 0.530 - 0.541\bar{s}_b + 0.429\bar{s}_b^2 - 0.171\bar{s}_b^3 \\ \alpha &= -0.571 - 0.803\bar{s}_b + 0.371\bar{s}_b^2 \\ \beta &= 1.980 + 0.308\bar{s}_b + 0.298\bar{s}_b^2 - 0.035\bar{s}_b^3 \end{aligned} \tag{15}$$

- $D_g^{(K^0+\overline{K}^0,\mathrm{NLO})}(x,Q^2)$:

$$\begin{aligned} N &= 0.330 - 0.307\bar{s} + 0.075\bar{s}^2 \\ \alpha &= -0.351 - 0.040\bar{s} - 0.282\bar{s}^2 + 0.033\bar{s}^3 \\ \beta &= 0.650 + 2.141\bar{s} - 0.457\bar{s}^2 + 0.075\bar{s}^3 \\ \gamma &= 1.096\bar{s} - 0.198\bar{s}^2 \end{aligned} \tag{16}$$

References

[1] J. Binnewies, B.A. Kniehl, and G. Kramer, Report Nos. DESY 95–048, MPI/PhT/95–20, and hep–ph/9503464 (March 1995), submitted to Phys. Rev. D.

[2] ALEPH Collaboration, D. Buskulic *et al.*, Z. Phys. C **64**, 361 (1994).

[3] DELPHI Collaboration, P. Abreu *et al.*, CERN–PPE/94–130, submitted to Z. Phys. C.

[4] OPAL Collaboration, R. Akers *et al.*, CERN–PPE/95–024, submitted to Z. Phys. C.

[5] L3 Collaboration, M. Acciarri *et al.*, Phys. Lett. B **328**, 223 (1994).

[6] MARK II Collaboration, H. Schellman *et al.*, Phys. Rev. D **31**, R3013 (1985).

[7] F.M. Borzumati, B.A. Kniehl, and G. Kramer, Z. Phys. C **57**, 595 (1993).

[8] F.M. Borzumati, B.A. Kniehl, and G. Kramer, Z. Phys. C **59**, 341 (1993); M. Greco, S. Rolli, and A. Vicini, *ibid.* **65**, 277 (1995).

[9] B.A. Kniehl and G. Kramer, Z. Phys. C **62**, 53 (1994); L.E. Gordon, Phys. Rev. **50**, 6753 (1994).

[10] G.D. Cowan, in *Proceedings of the XXVII International Conference on High Energy Physics*, Glasgow, Scotland, July 21–27, 1994, edited by P. Bussey and I. Knowles (World Scientific, Singapore, 1995).

[11] J. Binnewies, B.A. Kniehl, and G. Kramer, Z. Phys. C **65**, 471 (1995).

[12] F. Linsel, Doctoral Thesis, University of Hamburg (May 1995); private communication.

[13] UA5 Collaboration, G.J. Alner *et al.*, Nucl. Phys. **B258**, 505 (1985); UA5 Collaboration, R.E. Ansorge *et al.*, Z. Phys. C **41**, 179 (1988).

[14] CDF Collaboration, F. Abe *et al.*, Phys. Rev. D **40**, R3791 (1989); M.H. Schub, Ph.D. thesis, Purdue University, West Lafayette, Indiana (August 1989).

[15] M. Greco and S. Rolli, FNAL Report Nos. FERMILAB–PUB–94/324–A and hep–ph/9409356 (September 1994); S. Rolli, private communication.

[16] F. Aversa, P. Chiappetta, M. Greco, and J.Ph. Guillet, Phys. Lett. B **210**, 225 (1988); *ibid.* **211**, 465 (1988); Nucl. Phys. **B327**, 105 (1989).

[17] P. Aurenche, R. Baier, A. Douiri, M. Fontannaz, and D. Schiff, Nucl. Phys. **B286**, 553 (1987).

[18] G. Altarelli, R.K. Ellis, G. Martinelli, and S.Y. Pi, Nucl. Phys. **B160**, 301 (1979); R. Baier and K. Fey, Z. Phys. C **2**, 339 (1979).

[19] MINUIT, CERN Computer Centre Program Library.

[20] Particle Data Group, L. Montanet *et al.*, Phys. Rev. D **50**, 1173 (1994).

[21] CELLO Collaboration, H.J. Behrend *et al.*, Z. Phys. C **46**, 397 (1990).

[22] TASSO Collaboration, W. Braunschweig *et al.*, Z. Phys. C **47**, 167 (1990).

[23] HRS Collaboration, S. Abachi *et al.*, Phys. Rev. D **41**, 2045 (1990).

[24] TPC Collaboration, H. Aihara *et al.*, Phys. Rev. Lett **53**, 2378 (1984).

[25] CLEO Collaboration, S. Behrends *et al.*, Phys. Rev. D **31**, 2161 (1985).

[26] ARGUS Collaboration, H. Albrecht *et al.*, Z. Phys. C **44**, 547 (1989).

FIGURE CAPTIONS

Figure 1: x dependence of the NLO set of $K^0 + \overline{K}^0$ FF at $Q^2 = 100$ GeV^2.

Figure 2: Differential cross sections of inclusive $K^0 + \overline{K}^0$ production at LO (dashed lines) and NLO (solid lines) as functions of x at $\sqrt{s} = 91.2$ and 29.0 GeV. The theoretical calculations are compared with the respective experimental data by ALEPH [2] and MARK II [6]. For better separation, the distributions at 29.0 GeV have been divided by 10.

Figure 3: The (preliminary) p_T spectrum of inclusive K_S^0 production in ep collisions as measured by H1 [12] is compared with the NLO calculation in the $\overline{\text{MS}}$ scheme with $N_f = 5$ flavours using the photon and proton PDF of Refs. [27] and [28], respectively, together with our FF. The dashed/solid/dash-dotted curves correspond to the choices $\xi = 0.5/1/2$.

Figure 4: The p_T spectra of inclusive K_S^0 production in $p\bar{p}$ collisions as measured by UA5 [13] at $\sqrt{s} = 900$, 546, and 200 GeV are compared with the respective NLO calculations in the $\overline{\text{MS}}$ scheme with $N_f = 5$ flavours using the proton and antiproton PDF of Ref. [28]. For better separation, the spectra have been separated by factors of 10. The dashed/solid/dash-dotted curves correspond to the choices $\xi = 0.5/1/2$.

Figure 5: Same as Fig. 4, but for data from CDF [14] at $\sqrt{s} = 1800$ and 630 GeV.

Figure 6: Percentage of events with gluon fragmentation in the p_T spectra of K_S^0 mesons inclusively produced in $p\bar{p}$ and ep collisions. The solid, dash-dotted, dashed, and dotted lines represent our predictions for the 1800 GeV and 630 GeV CDF [14], 200 GeV UA5 [13], and H1 [12] experiments, respectively.

Figure 7: Ratio of the differential cross section for inclusive kaon production to that for charged hadrons as a function of p_T. We compare the $p\bar{p}$ data on K_S^0 mesons by CDF [14] and the pp data on K^+ and K^- mesons (averaged) by the British-Scandinavian (BS) [30] and Chicago-Princeton (CP) [31] Collaborations with the respective NLO calculations using our FF. We compute the denominators by summing over the charged pions and kaons.

[27] M. Glück, E. Reya, and A. Vogt, Phys. Rev. D **46**, 1973 (1992).

[28] H.L. Lai, J. Botts, J. Huston, J.G. Morfin, J.F. Owens, J.W. Qiu, W.K. Tung, and H. Weerts, Phys. Rev. D **51**, 4763 (1995); W.K. Tung, private communication.

[29] F.M. Borzumati and G. Kramer, Report Nos. DESY 95–020, TUM–T31–84/95, and hep–ph/9502280 (January 1995).

[30] British-Scandinavian Collaboration, B. Alper *et al.*, Nucl. Phys. **B100**, 237 (1975).

[31] Chicago-Princeton Collaboration, D. Antreasyan *et al.*, Phys. Rev. D **19**, 764 (1979).

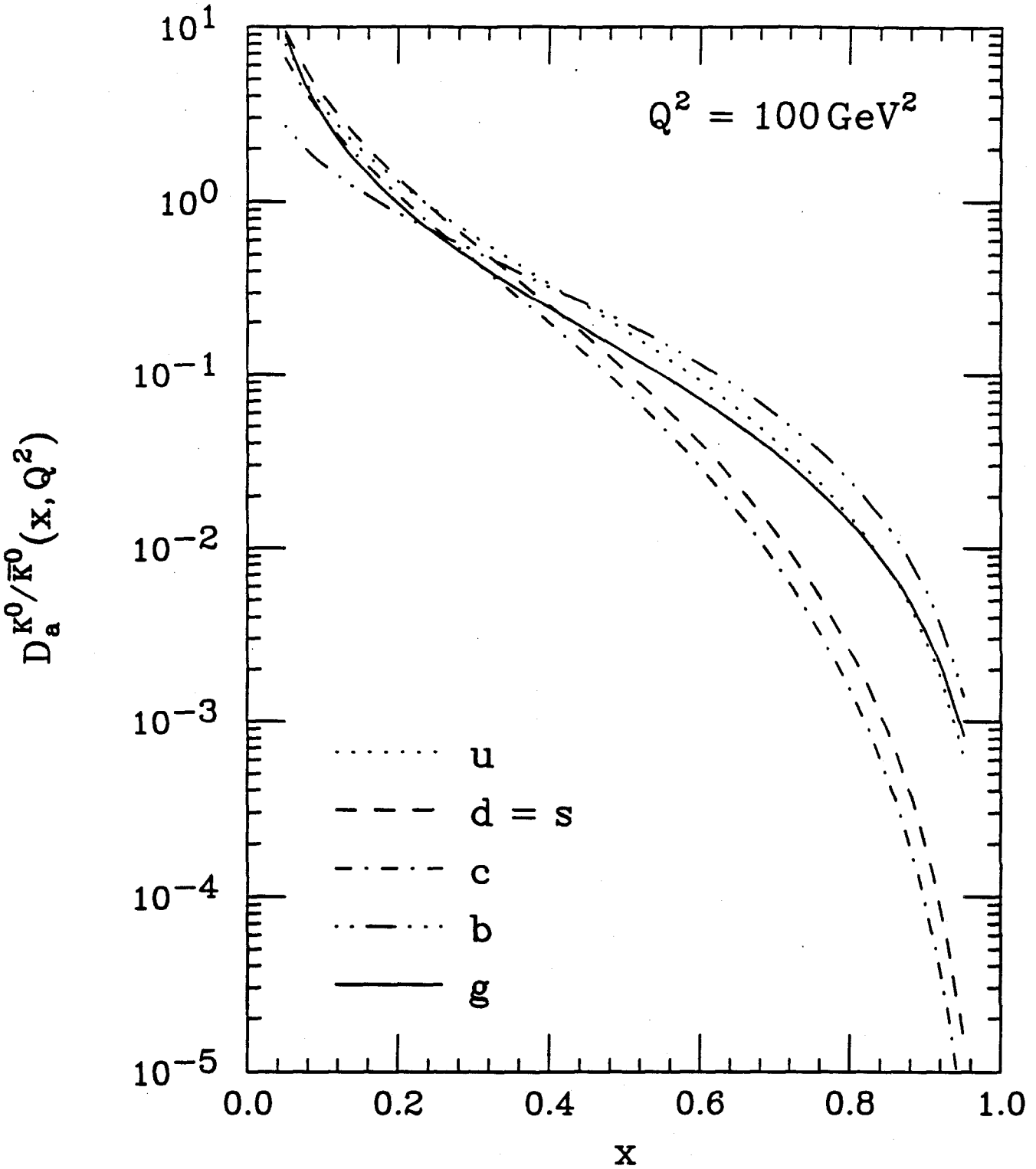
$Q^2 = 100\,\mathrm{GeV}^2$
$D_a^{K^0/\bar{K}^0}(x, Q^2)$
10^1
10^0
10^{-1}
10^{-2}
10^{-3}
10^{-4}
10^{-5}
0.0
0.2
0.4
0.6
0.8
1.0
x
u
d = s
c
b
g

Fig. 1

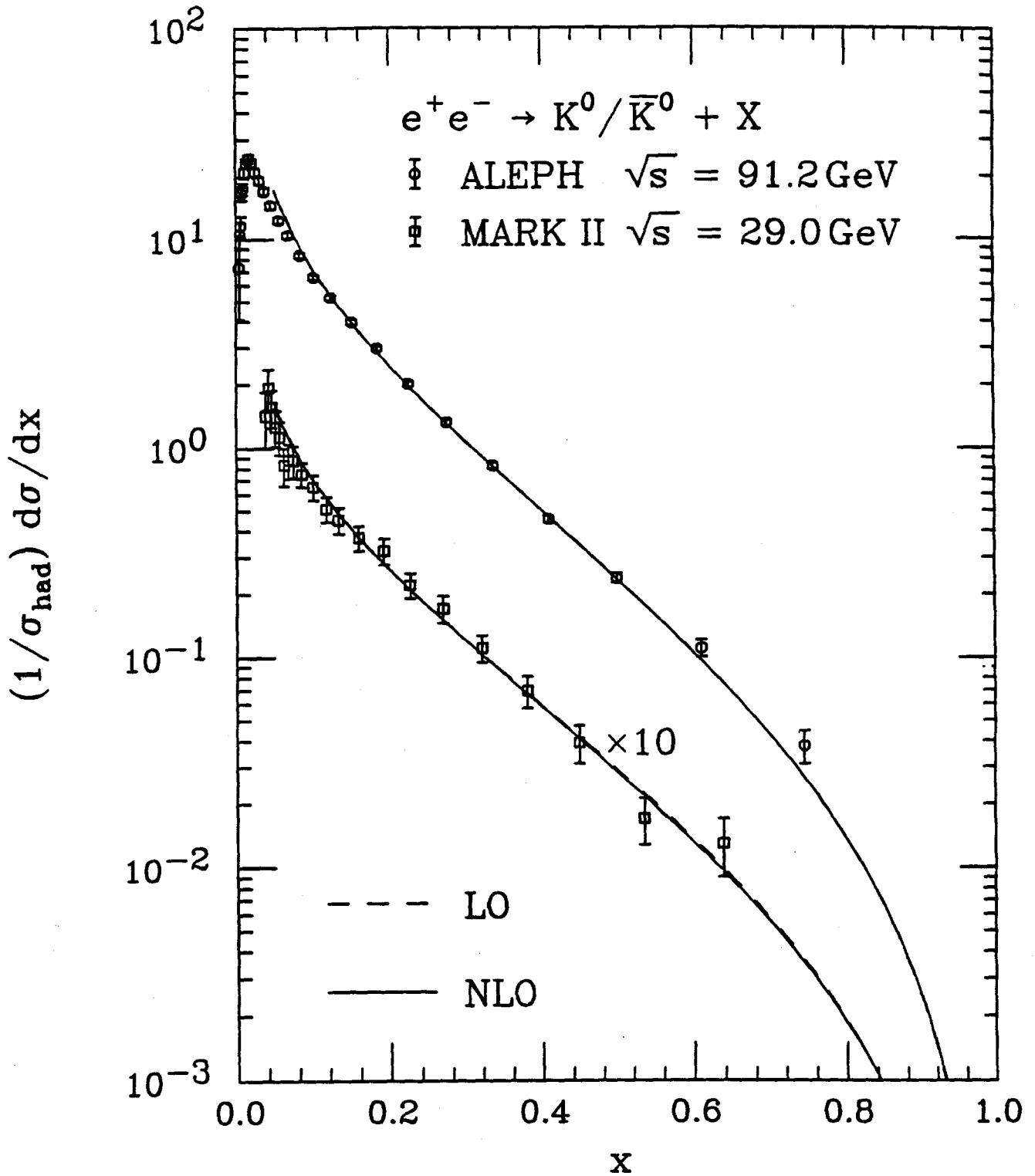
$e^+e^- \to K^0/\overline{K}^0 + X$
ALEPH $\sqrt{s}$ = 91.2 GeV
MARK II $\sqrt{s}$ = 29.0 GeV
×10
LO
NLO
$(1/\sigma_{had})\, d\sigma/dx$
x
10^2
10^1
10^0
10^{-1}
10^{-2}
10^{-3}
0.0
0.2
0.4
0.6
0.8
1.0

Fig. 2

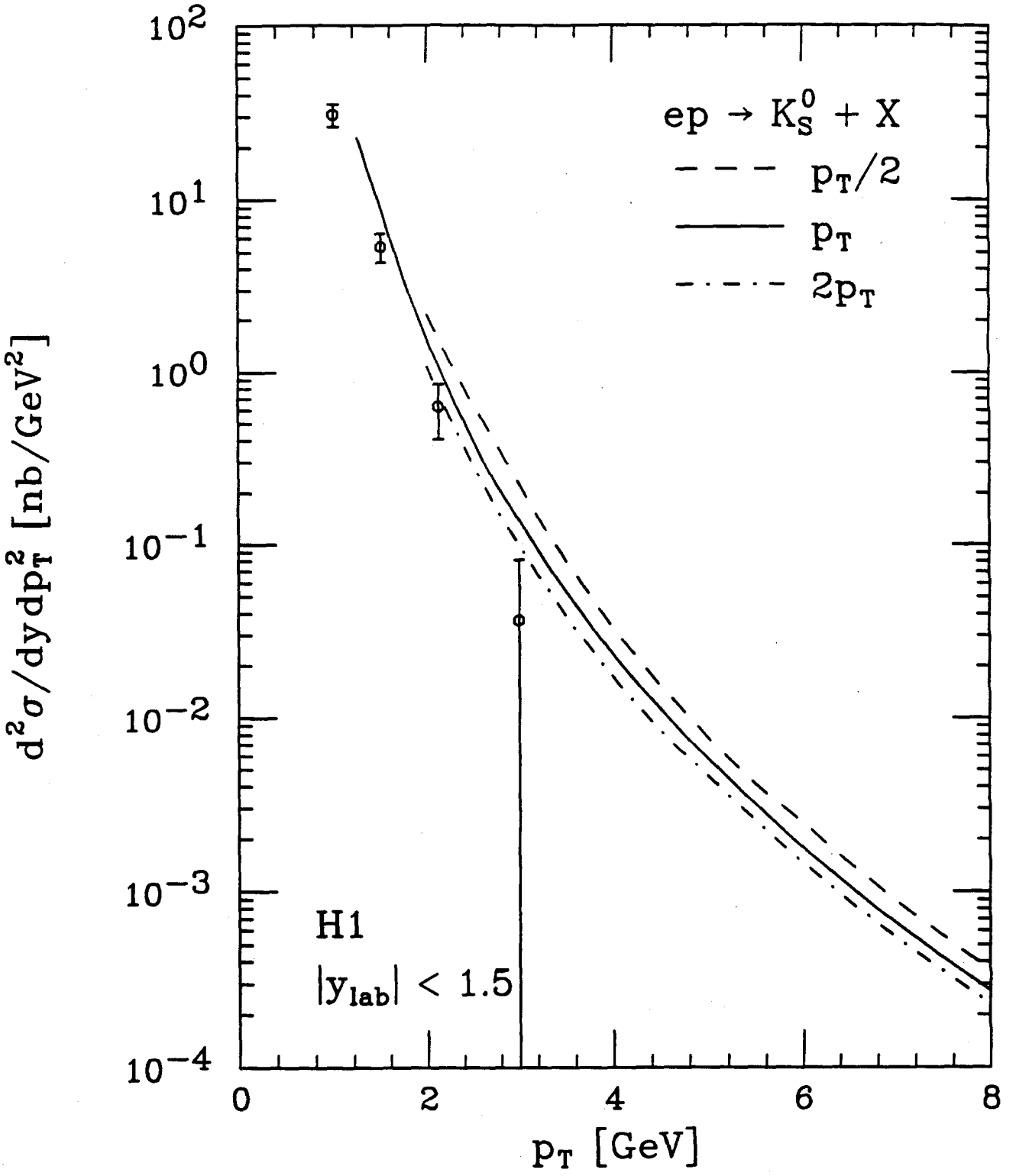
$ep \to K_S^0 + X$
$p_T/2$
p_T
$2p_T$
H1
$|y_{lab}| < 1.5$
$d^2\sigma/dy\,dp_T^2$ [nb/GeV^2]
p_T [GeV]
10^2
10^1
10^0
10^{-1}
10^{-2}
10^{-3}
10^{-4}
0
2
4
6
8

Fig. 3

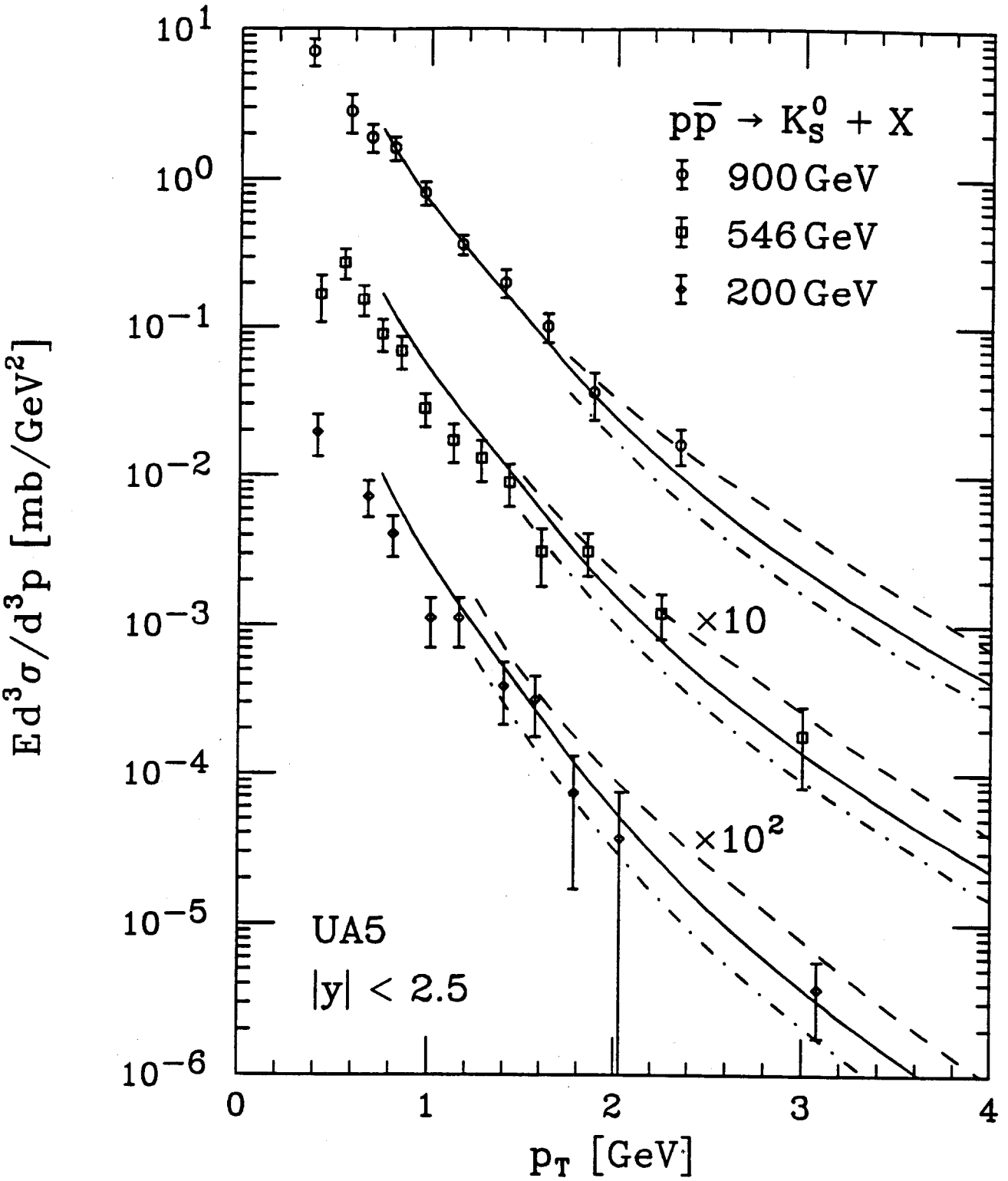
$p\bar{p} \to K_S^0 + X$
900 GeV
546 GeV
200 GeV
×10
×10²
UA5
|y| < 2.5
$Ed^3\sigma/d^3p$ [mb/GeV²]
p_T [GeV]
10¹
10⁰
10⁻¹
10⁻²
10⁻³
10⁻⁴
10⁻⁵
10⁻⁶
0
1
2
3
4

Fig. 4

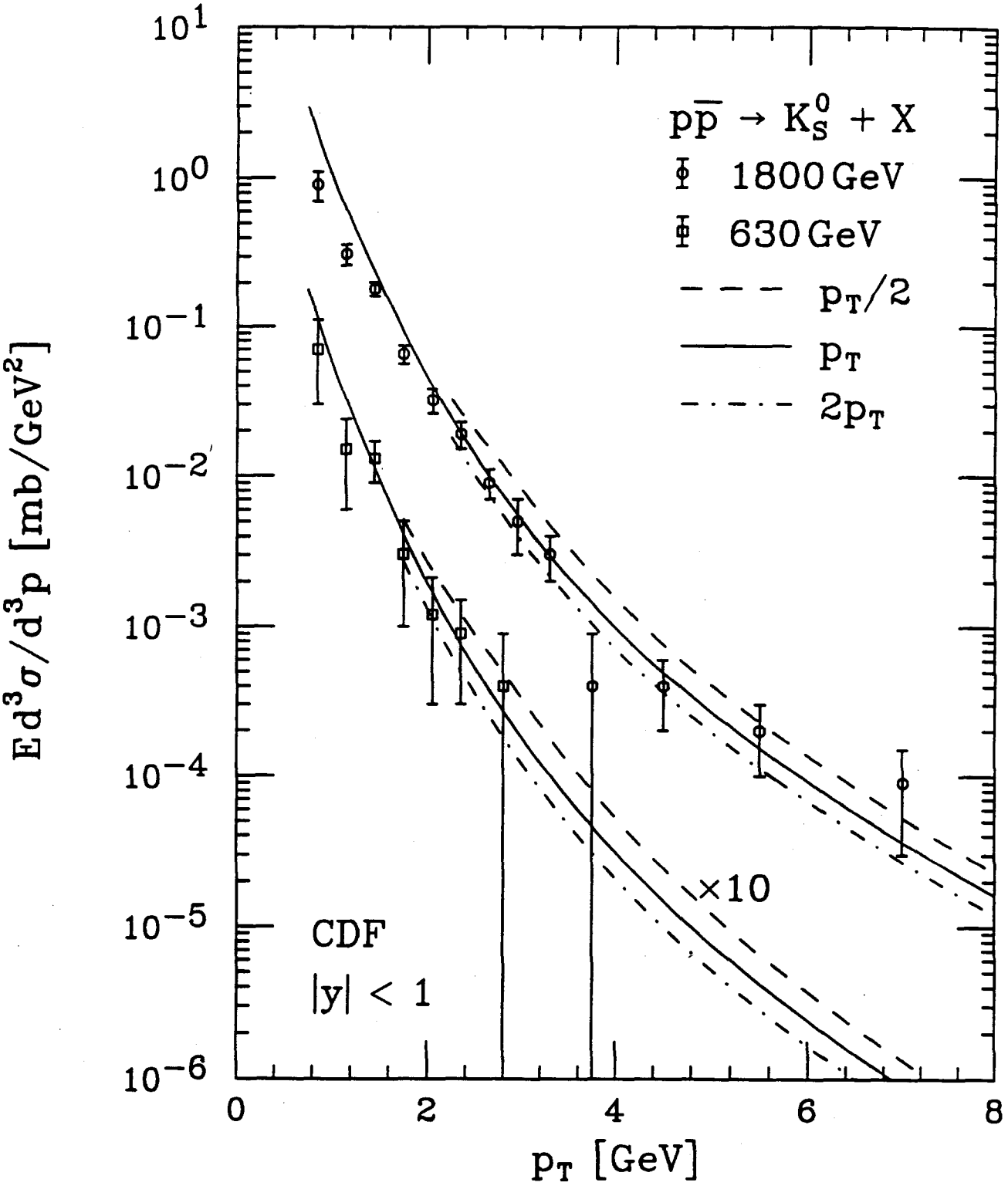
$p\bar{p} \to K_S^0 + X$
1800 GeV
630 GeV
$p_T/2$
p_T
$2p_T$
×10
CDF
$|y| < 1$
$Ed^3\sigma/d^3p$ [mb/GeV^2]
p_T [GeV]
10^1
10^0
10^{-1}
10^{-2}
10^{-3}
10^{-4}
10^{-5}
10^{-6}
0
2
4
6
8

Fig. 5

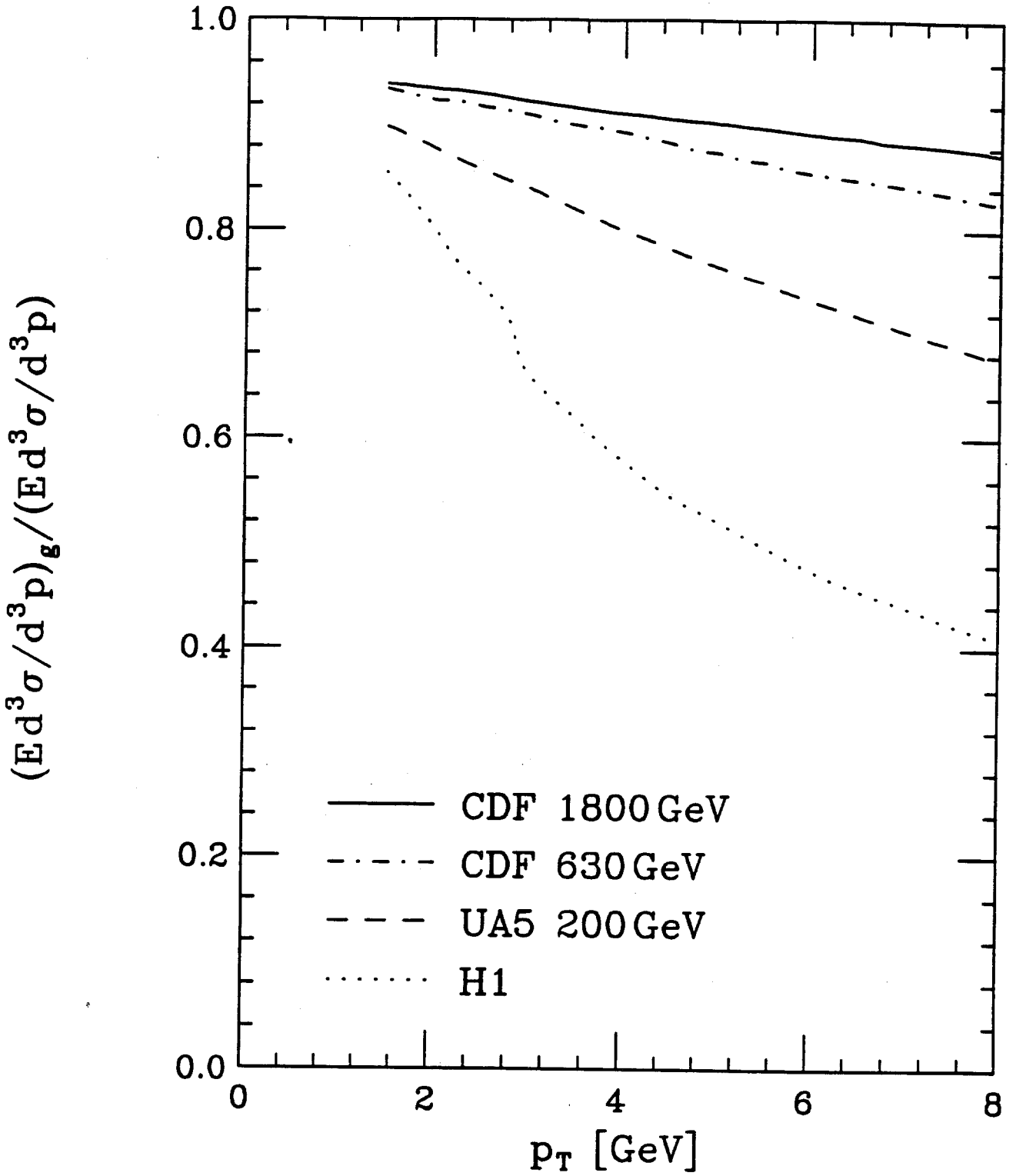
1.0
0.8
0.6
0.4
0.2
0.0
0
2
4
6
8
$(Ed^3\sigma/d^3p)_g/(Ed^3\sigma/d^3p)$
p_T [GeV]
CDF 1800 GeV
CDF 630 GeV
UA5 200 GeV
H1

Fig. 6

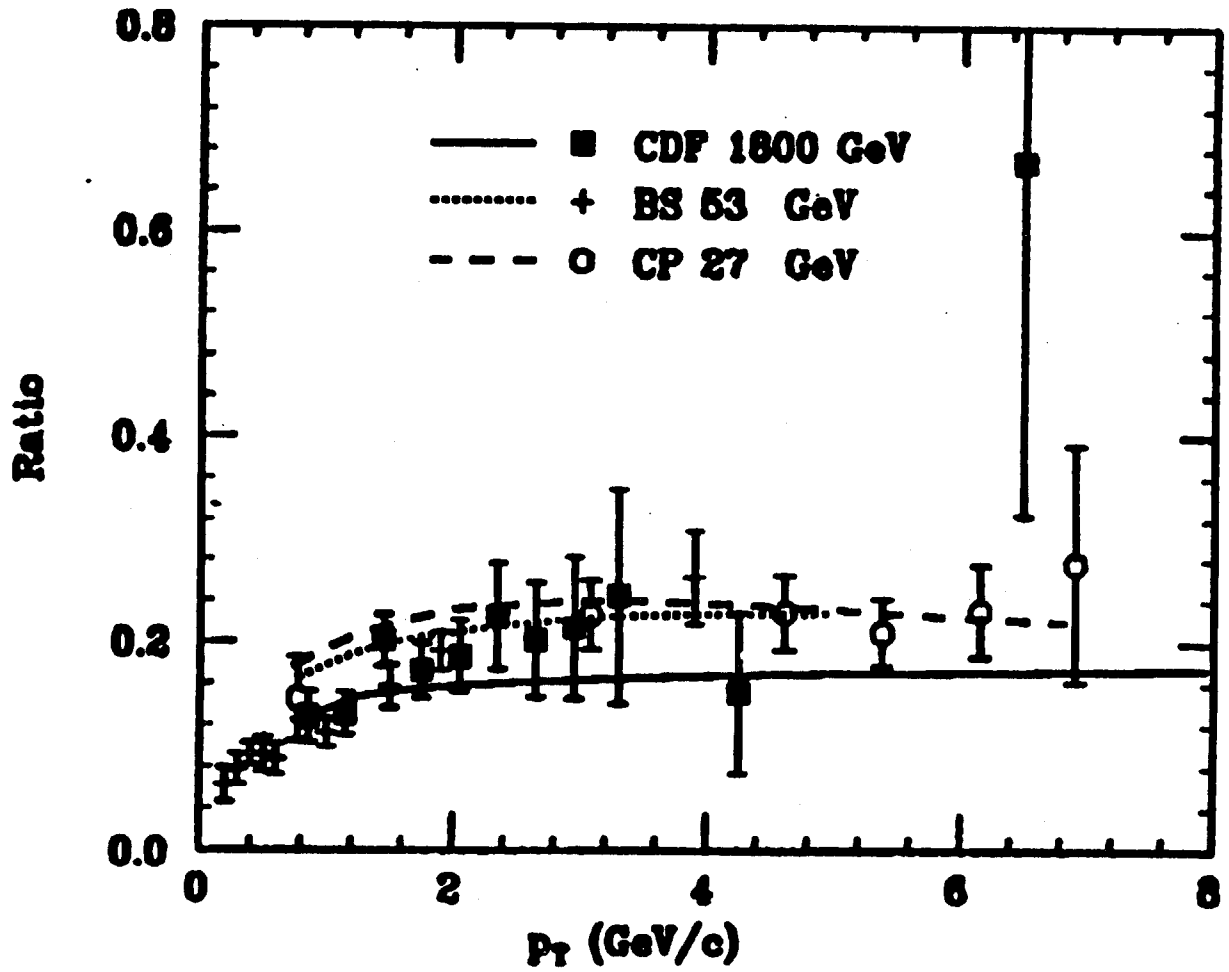
CDF 1800 GeV
BS 53 GeV
CP 27 GeV
Ratio
0.0
0.2
0.4
0.6
0.8
0
2
4
6
8
p_T (GeV/c)

Fig. 7